Renewable Energy 202 (2023) 865–879

Contents lists available at ScienceDirect

Renewable Energy

journal homepage: www.elsevier.com/locate/renene

# Numerical analyses of energy screw pile filled with phase change materials

Wenbin Fei [a,*], Luis A. Bandeira Neto [a], Sheng Dai [b], Douglas D. Cortes [c], Guillermo A. Narsilio [a]

[a] Department of Infrastructure Engineering, The University of Melbourne, Parkville, Australia
[b] School of Civil and Environmental Engineering, Georgia Institute of Technology, Atlanta, GA, 30332, USA
[c] Civil Engineering Department, New Mexico State University, Las Cruces, NM, 88003, USA

ARTICLE INFO

*Keywords:*
Geothermal engineering
Energy pile
Screw pile
Phase change material
Ground source heat pump

ABSTRACT

Embedding heat exchangers into a screw pile can form a cost-effective energy pile with a fast installation capability. However, better solutions to handle thermal waves and thermal interferences among energy piles are still required. This work aims to solve the issues by proposing a novel concept of an energy screw pile filled with mixtures of phase change materials (PCM) such as paraffin and "solid" grouting. Numerical simulations are conducted to investigate the utilisation of PCM energy screw piles on reducing fluid and ground temperatures, considering different constituents in PCM-solid mixtures, moisture conditions, phase change temperatures $T_{pc}$ and operation schemes. Results demonstrate that a mixture with higher effective thermal conductivity $\lambda_{eff}$ slows down the PCM phase transition and results in a lower fluid temperature feeding the ground source heat pump (GSHP). Dry mixtures with higher PCM content benefit the fluid temperature reduction, while a lower PCM content in a wet mixture is also satisfactory. Higher specific heat capacity allows pile back-filling to absorb more heat and reduce the thermal radius of influence, while over-enhancing its $\lambda_{eff}$ might worsen thermal interference. The selection of the PCM phase change temperature $T_{pc}$ should comply with the GSHP system operation scheme and the project aim.

## 1. Introduction

Seeking renewable energy to reach a carbon-neutral society by 2050 or even earlier has become a priority for many countries [1]. Heat stored within the Earth is an ample renewable energy resource and it has the merit of constant 24/7 availability regardless of the weather conditions. Ground source heat pumps (GSHPs) utilise water pipes embedded in the soil as a ground heat exchanger (GHE) medium to inject/absorb heat into/from the ground for aboveground space cooling in summer and heating in winter. Since the ground temperature is relatively constant below a certain depth compared to the variational ambient air temperature above the ground, GSHPs are more efficient than conventional systems such as air conditioners and gas burners [2]. Existing research has demonstrated that GSHPs can supply up to six times as much as the (electric) energy used as input power for the systems, i.e. they render a coefficient of performance (COP) of up to typically six [3]. However, the wide adoption of GSHPs is impeded by their high capital costs. Borehole drilling is required to place water pipes in a vertical GSHP system and the associated drilling costs could account for 50% of the upfront cost for a project since drilling is priced by depth [4].

To reduce capital costs, the concept of energy geo-structure was introduced by embedding water pipes into structures such as piles, tunnels and retaining walls [5–7]. Among these energy geo-structures, energy piles have dual functions: not only as heat exchangers but also as structural elements bearing loads from buildings. As drilling work is a part of pile construction, energy piles can eliminate the costs of separate drilling for conventional vertical GSHP systems, resulting in an approximately 30% cost reduction [4]. Embedding GHEs into piles also saves the required space for the borehole system [8,9]. However, energy piles implementation is still facing other technical challenges.

Firstly, in the short term (hours or days), since the ground thermal response is much slower than the heat pump requirement, the start-stop of a heat pump generates thermal waves and soil temperature fluctuations. This delayed response of the ground could lower the coefficient of performance (COP) of the GSHP because the peaks of the thermal wave might require a large heat flux that could exceed the capacity of the heat pump [10,11]. Secondly, in the medium-term (weeks to months), the thermal radius of influence around the energy piles usually exceeds the distance between two neighboring piles since the pile spacing is primarily designed for transferring load from buildings to soil/rock layers

*Abbreviations:* PCM, Phase change material; GSHP, Ground source heat pump.

* Corresponding author. Engineering Block B 204a, Department of Infrastructure Engineering, The University of Melbourne, Parkville, VIC, 3010, Australia
*E-mail address:* wenbinfei@outlook.com (W. Fei).

https://doi.org/10.1016/j.renene.2022.12.008
Received 30 August 2022; Received in revised form 21 November 2022; Accepted 3 December 2022
Available online 4 December 2022

rather than thermal efficiency. The large thermal radius might lead to thermal interference between piles and thus a low efficient geothermal system [12,13]. At last, in a long term (months to years), the extracted/injected heat is meant to be recovered by reversed injection/extraction in the later seasons under a designed balanced thermal load. However, the actual thermal load is typically seasonally imbalanced in heating/cooling dominated buildings, resulting in an accumulated increase/decrease in the ground temperature [10–12]. Qian and Wang [14] concluded that soil temperature could decrease by 10.6 °C and the COP decrease by 0.25 after 10 years of a constant cooling load of 50 kW. In contrast, soil temperature can increase by 12.5 °C and the COP can decrease by 1.25 after 10 years of a constant heating load of 50 kW. This long-term thermal imbalance will not only decrease the resulting COP of energy pile foundations but could also cause system failure before the expected lifespan if not properly designed.

To address the aforementioned technical issues, several solutions were proposed including (i) increasing the pile length, (2) constructing more piles, (3) coupling supplementary devices such as boilers [15,16] and ice storage tanks [17,18], and/or (4) incorporating thermal energy storage (TES) system [19]. The first three proposals will increase the upfront construction and operation cost substantially and may not be even feasible depending on geological conditions, while the TES system could be an appropriate solution since phase change materials (PCMs) used in the system can store and release latent heat energy at a constant temperature [11,20].

PCMs have a wide application in infrastructure engineering. They have been implemented in building wall-boards, concrete, floors, gypsum and other parts for passive thermal control [21]. They have also been used to develop thermal batteries to replace the lithium-ion battery to store energy for solar power plants since their energy storage capability will not be degraded over time [22,23]. According to the phase state before and after phase change, PCMs can be classified into solid-solid, solid-liquid, solid-gas and liquid-gas PCMs. For a solid-liquid PCM, its temperature can increase until reaching the phase change temperature, then transform from solid to liquid state while keeping the temperature constant, due to the release of latent heat. Solid-liquid PCMs are the most commonly used PCMs due to their large latent heat capacity and low volume change during phase transition [24,25].

In GSHP or shallow geothermal systems, PCMs have been employed as backfill materials for borehole applications to improve the COP of geothermal systems [12,26]. Since liquid PCMs could be lost in boreholes and contaminate the subsurface environment, PCMs are reacted with other substances such as polyethylene or silica to form shape-stabilized PCM mixtures [27,28]. Alternatively, PCMs can be encapsulated in shells to prevent their leakage when at the liquid state and dampen volume change at melting [25,29]. To improve the general low thermal conductivity of PCMs, additives with high thermal conductivity such as metal, graphite and carbon fibre can also be added to PCMs [30]. Encapsulation also improves the thermal conductivity of PCMs due to the increase in the continuity of heat transfer pathways and surface area [31]. By applying these enhancement methods, PCM-modified soils/grouts are introduced into borehole GSHPs as backfill materials to reduce the working fluid temperature and decrease the thermal radius [32,33]. Li et al. [34] introduced a shape-stabilized phase change backfill material that is made of capric/lauric acid with 10% of silica and 6% of expanded graphite. Replacing the crushed stone backfill with this PCM-modified material can increase the heat transfer rate by 23% and reduce the thermal radius by 10%. Dehdezi et al. [35] demonstrated that using microencapsulated PCM-modified soils as backfill materials can reduce the ground temperature by 3 °C and improve the COP of GSHP by more than 17%. In addition, the thermal wave in the ground can be smoothed with the implementation of PCM-modified backfill [26]. However, using the PCM-modified backfill in borehole geothermal systems does not eliminate the drilling costs.

Compared with many studies related to PCM-modified backfills, very few works have incorporated PCMs into energy piles. Inspired by the concept of dispersing PCMs in concrete mixtures in the building industry [36–38], Han et al. [39] proposed to incorporate encapsulated PCM particles into the concrete energy piles for bridge deck snow melting. Their numerical results showed the employment of PCM into concrete piles enhanced the geothermal energy extraction significantly. Another concept that embedding PCM containers into the concrete shell of energy piles was introduced by Mousa et al. [40]. The utilisation of PCM resulted in lower temperature distribution than that of its peers without PCM. However, adding the PCM into concrete might lower the compressive capacity of the concrete since PCMs are generally soft, which also limited the employment of a large amount of PCMs into concrete. Therefore, it is of great importance to propose new PCM-enhanced energy piles.

This paper proposes a novel concept of energy screw pile coupled with PCM, as shown in Fig. 1. Commercial screw piles are utilised in the construction industry for building foundation anchoring. They are made of steel with helical heads to drill through ground formations including soil, gravel and bedrocks [41]. They usually have a length of 10–25 m and they are well known for their quick installation and low installation costs since no special specialized drilling equipment and expertise are required [42]. The study of using screw piles as GHEs to harvest geothermal energy is at an early stage, and incorporating PCM into screw piles is a unique and novel work that needs to be explored [41,43].

Since screw piles have close-ends, either normal or encapsulated PCMs can be mixed with sands as back-filling s to be added into the piles without the concern of leaking to the underground environment. Filling PCM-sand mixtures are expected to save more construction time than conventional grouting. Three types of mixtures including PCM-sand (PS), PCM-demolished concrete (PC) and PCM mixed with an equal volume of sand and demolished concrete (PSC) were considered as the screw pile fillings in this work. The employment of demolished concrete also contributes to the recycling society and carbon emission reduction. For each type of the mixtures, three different volume fractions of PCM (10%, 20% and 30%) were considered. The effects of different mixtures, phase change materials and thermal loading schedules on the working fluid temperature and thermal radius were investigated in this work.

## 2. Numerical model of energy screw pile system

A numerical model of a screw pile filled with concrete was first validated by an in-situ Thermal Response Test (TRT) test executed in a group of eight energy screw piles in Melbourne, Australia (Fig. 1). Further details of such test can be found in Bandeira-Neto et al. [44]. To

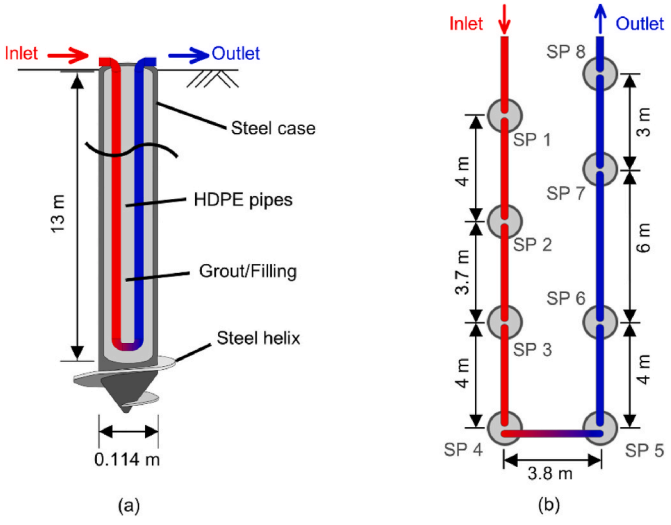


**Fig. 1.** A typical energy screw pile: schematic vertical cross section (a), and plan view of the screw pile group in Melbourne (b).

assess this prototype of the PCM energy screw pile (i.e., pile filling in Fig. 1 is PCM), the validated model was modified to consider only a single pile under three thermal loading schemes: (i) constant heating, (ii) intermittent heating, and (iii) realistic thermal loading.

### 2.1. Geometry and boundary conditions

A rectangular prism of 28 m × 23.8 m × 23 m and a cylinder with a diameter of 20 m and a height of 28 m were built in COMSOL Multiphysics [45] to represent the geometries of soil body and a single pile, respectively, as shown in Fig. 2. The eight piles in the group were distributed as presented in Fig. 1 in the centre of the rectangular prism while a single PCM energy screw pile was located in the centre of the soil body. The screw pile made of steel with a wall thickness of 7.1 mm and a flat helix with as diameter of 350 mm was explicitly considered in the model since steel has a high thermal conductivity. According to the screw piles design of a real operational project in Melbourne, the pile had a diameter of 114 mm and a length of 13 m (Fig. 1), with a single U-loop HDPE pipe installed in the pile. The inner diameter and wall thickness of the HDPE pipe were 26.9 and 2.3 mm, respectively. One-dimensional elements were used to simulate the non-isothermal flow in the HDPE pipe. The ambient temperature recorded during the in-situ TRT test was assigned to the ground surface in the validation model since no building was constructed over the pile during the test, while the ground surface was considered to be adiabatic for simulating the single screw pile during the operation period in which the buildings would have been constructed. The side and bottom of the model were given a constant far-field temperature of 18 °C [46] on both geometries for simplicity.

### 2.2. Governing equations

The numerical models coupled governing equations of heat transfer and fluid flow. Heat conduction was considered in all solid materials (i.e., ground, steel case, pile back-filling and pipe wall) while both conduction and convection were contemplated for the circulating fluid. There is no groundwater flow on site at the relevant depths. Fluid was considered incompressible and the fluid flow modelling is based on the momentum (Eq. (1)) and continuity (Eq. (2)) equations. The conductive-convective heat transfer within the carrier fluid was given by Eqs. (3) and (4), and the heat conduction on the solid materials was computed using Eq. (5). These equations were included in the modules of "Non-isothermal Pipe Flow" and "Heat Transfer in Porous Media" in COMSOL Multiphysics [45].

$$A\rho_f \nabla \bullet \boldsymbol{v} = 0 \tag{1}$$

$$\rho_f \left(\frac{\partial \boldsymbol{v}}{\partial t}\right) = -\nabla p - f_D \frac{\rho_f}{2d_h} \boldsymbol{v}|\boldsymbol{v}| \tag{2}$$

$$\rho_f A C_{p,f} \frac{\partial T_f}{\partial t} + \rho_f A C_{p,f} \boldsymbol{v} \bullet \nabla T_f = \nabla \bullet \left(A\lambda_f \nabla T_f\right) + f_D \frac{\rho_f A}{2d_h} |\boldsymbol{v}|\boldsymbol{v}^2 + Q_{wall} \tag{3}$$

$$Q_{wall} = f\left(T_{pipe\ wall}, T_f, \lambda_p, d_p\right) \tag{4}$$

$$\rho_m C_{p,m} \frac{\partial T_m}{\partial t} = \nabla \bullet \left(\lambda_m \nabla T_m\right) \tag{5}$$

where $A$ is the inner cross-section of the HDPE pipes, $\rho_w$ is the carrier fluid density, $v$ is the fluid velocity vector field, $t$ is the time, $p$ is the pressure, $f_D$ represents the Darcy friction factor, $d_h$ is the hydraulic diameter of the pipe. $C_{p,f}$ represents the fluid's specific heat capacity, $\lambda_f$ is the fluid thermal conductivity. $Q_{wall}$ stands for the external heat exchange rate through the pipe wall, and is a function of the temperature on the pipe outer wall ($T_{pipe\ wall}$), the fluid temperature ($T_f$), the pipe wall thermal conductivity and the pipe diameter. $\rho_m$ is the material density, $C_{p,m}$ is the material specific heat capacity, $T_m$ is the material temperature field and $\lambda_m$ is the thermal conductivity of the material. Further details of this model can be found in Bidarmaghz [47] and in Makasis [48].

To incorporate the PCM phase change in the model, the heat conduction equation needs to be modified in a similar fashion as in Lu et al. [49]. Therefore, the apparent heat capacity method is used, considering both sensible and latent heat added when the phase change process is underway. When a PCM material is introduced, Equation (5) becomes (6), with the material heat capacity given by $C_{p,PCM}$, and the material thermal conductivity, by $\lambda_{PCM}$:

$$\rho_{PCM} C_{p,PCM} \frac{\partial T_m}{\partial t} = \nabla \bullet \left(\lambda_{PCM} \nabla T_m\right) \tag{6}$$

$$C_{p,PCM} = \left(\theta_1 C_{p,ph1} + \theta_2 C_{p,ph2}\right) + L\frac{\partial m_i}{\partial T} \tag{7}$$

$$m_i = \frac{1}{2}\frac{\theta_2 - \theta_1}{\theta_1 + \theta_2} \tag{8}$$

$$\lambda_{PCM} = \theta_1 \lambda_{ph1} + \theta_2 \lambda_{ph2} \tag{9}$$

$$\theta_1 + \theta_2 = 1 \tag{10}$$

where $\rho_{PCM}$ is the PCM material density. Despite the fact that the PCM density value changes between solid and liquid phases, the model needs a constant value to ensure the conservation of mass, so an average thermal value is considered. $\theta_1$ and $\theta_2$ are the phase indicators (volume fraction) representing the solid phase and liquid phases respectively. In

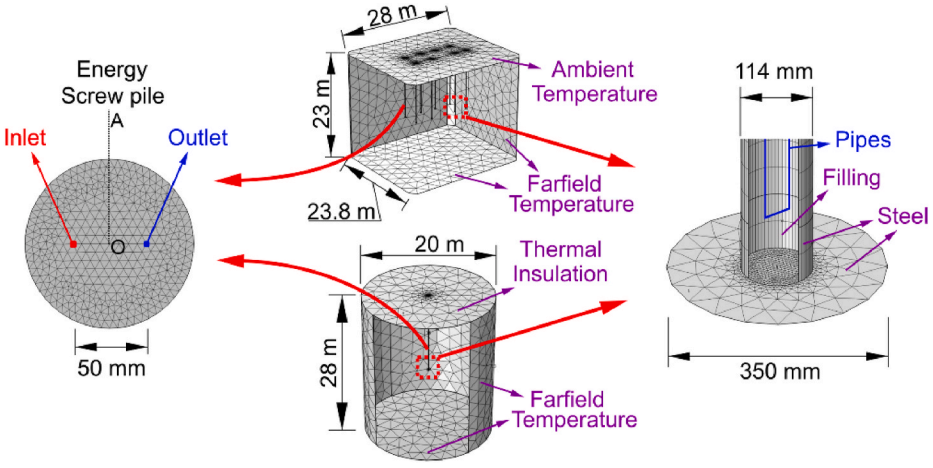


**Fig. 2.** Geometry, key boundary conditions of the finite element model for the 13-m-deep piles – group and single pile geometries.

addition, $C_{p,ph1}$ and $C_{p,ph2}$ are the specific heat capacities when the PCM is at solid and liquid phases, respectively, and $\lambda_{ph1}$ and $\lambda_{ph2}$ are the associated thermal conductivity. $L$ is the latent heat of fusion. As shown in Fig. 3, the material changes phase when the phase change temperature ($T_{pc}$) is reached. The model assumes that PCM has a phase change temperature range $\Delta T_{pc}$, so the phase transformation starts at $T_{pc}$ - $\Delta T_{pc}$/2 and finishes at $T_{pc} + \Delta T_{pc}$/2.

### 2.3. Model validation

An in-situ TRT was conducted on a group of eight energy screw piles using roughly 5.0 kW of heating power in Melbourne, Australia for over 66 h. The screw piles were filled with grout and its geometry is shown in Fig. 1. A sample of the grout was taken from the site and its thermal conductivity was tested to be 1.6 W/(m K) by using a thermal needle in the laboratory. The TRT test recorded the injected heat energy and associated temperature at the inlet and outlet, more details can be found in the paper [44].

For the model validation, the TRT test was simulated considering the original test conditions, using the inlet fluid temperature recorded in the in-situ test and ambient temperature shown in Fig. 4(a). The initial temperature of the water and undisturbed ground were 18 °C [46]. The corresponding material properties are summarised in Table 1. The numerical fluid temperature was compared with the in-situ experimental measurements in Fig. 4(b), and results show they have a good agreement with each other despite the numerical results being larger at the end of the test.

### 2.4. Numerical models with PCM

Instead of casting grout into the central hollow part of the screw pile, PCM-sand mixtures were employed in this new concept of energy screw pile to boost the construction speed and address the technical issues of energy piles. Pluviating pure sand particles into the pile without compaction can result in a large porosity of the back-filling, here assumed as 0.4. To increase both the heat storage and heat transfer capability, PCM is thought to be added into the voids of sand particle assemblies while not reducing the volumetric fraction of sand. Three volume fractions of PCM (10%, 20% and 30%) were used to (virtually) prepare the PCM-sand mixtures. Additionally, three types of sands were selected for the mixtures: (i) quartz sand, (ii) demolished concrete, also known as recycling sand, and (ii) an equal amount of quartz sand and demolished concrete. Both dry and saturated PCM-sand mixtures conditions were simulated in this work to investigate the associated effect on the performance of the novel energy screw pile. Table 2 presents the properties of the constituents and the equations used to calculate the thermal properties of PCM-sand mixtures. The material phase change temperature $T_{pc}$ determines the activation of the phase transition process; three $T_{pc}$ of 20, 25 and 30 °C were considered in the simulations. Since the group pile model was significantly larger and therefore demands more computational resources, in order to simulate all these back-filling materials the single pile model was used.

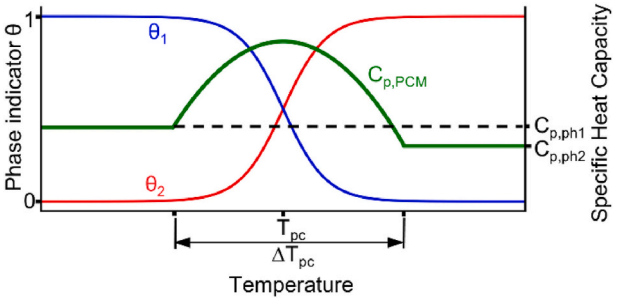


**Fig. 3.** Apparent heat capacity method. For a solid-liquid PCM, phase 1 is solid while phase 2 is liquid.

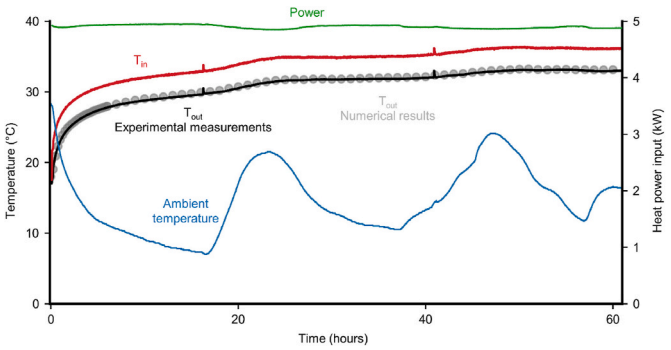


**Fig. 4.** Numerical model validation by experimental measurements in a group of piles with cementitious grout as backfilling material: key input parameters (power, fluid inlet temperature and ambient temperature), and results comparison between experimentally measured and numerically obtained outlet fluid temperature (b).

**Table 1**
Material properties used for model validation.

| Material | Density $\rho$ (kg/m$^3$) | Thermal conductivity $\lambda$ (W/m·K) | Specific heat capacity $C_p$ (J/kg·K) |
|---|---|---|---|
| Ground | 2000 | 1.5 | 830 |
| Grout | 2250 | 1.6 | 890 |
| Steel | 7850 | 44.5 | 475 |

**Table 2**
Properties of PCM-sand mixtures and their constituents.

| Material | Density $\rho$ (kg/m$^3$) | Thermal conductivity $\lambda$ (W/m·K) | Specific heat capacity $C_p$ (J/kg·K) | Latent Heat $LH$ (kJ/kg) |
|---|---|---|---|---|
| Quartz | 2650 | 7.70 | 740 | – |
| Demolished concrete | 2250 | 3.12 | 1060 | – |
| Paraffin PCM [50] | 771 | 0.36 ($s$)<br>0.15 ($l$) | 2222 | 243.5 |
| Water | 1000 | 0.60 | 4192 (10 °C) | – |
| Air (20 °C) | 0 | 0.03 | – | – |
| Mixture[a] | $\sum X_i f_i$ | $\prod X_i^{f_i}$ | $\frac{\sum X_i \rho_i f_i}{\sum \rho_i f_i}$ | $\frac{\sum X_i \rho_i f_i}{\sum \rho_i f_i}$ |

Note: $s$ stands for solid state while $l$ stands for liquid state. $I$ indicate the phase in the equations of the bottom row, $f$, $X$ and $\rho$ are the volumetric content, property value (thermal conductivity or specific heat) and density of the corresponding phase. The thermal properties of each mixture is summarised and presented in Appendix I.

## 3. Results and discussions

Several PCM-sand mixtures varying in components, PCM contents and $T_{pc}$ were involved in the *in-principle* validated numerical models under three different operation schemes to investigate the performance of the PCM-modified energy screw pile.

### 3.1. Constant heating injection

#### 3.1.1. Pile back-filling composition

The back-filling materials in the proposed PCM energy screw pile play two roles: (i) exchanging heat between the water pipes and the ground; and (ii) storing or releasing heat due to the unique thermal property of PCM. Since sands with relatively high thermal conductivities contribute more to heat transfer while PCM controls the heat storage/

release, the combinations of three types of sands and PCM following different proportions were tested in this work. A constant heating rejection load to the ground of 0.65 kW (average value employed per pile in the group TRT test) was used for 48 h, which represents a proportional constant building cooling load (i.e., air conditioning a building).

For the *dry* conditions PCM with the $T_{pc}$ of 25 °C, the mean fluid temperature $T_{f,mean} = (T_{in} + T_{out})/2$ and solid state variations that resulted from using three mixtures (i) 30% PCM-sand (30% PS), (ii) 10% PCM-sand (10% PS) and (iii) 30% PCM-concrete (30% PC) within 48 h were plotted in Fig. 5, alongside the energy screw pipe filled by grout as a reference. After operating the systems for 5 h, utilising 30% PS in the screw pile shows a consistent 2.5 °C lower temperature than that using 10% PS. The lower fluid temperature induced by the incorporation of PCM can reduce the working load of the heat pump and increase COP, presenting the potential advantage of using a heat pump with cooler entering water temperatures or removing the high peaks of the fluid temperature due to abnormal thermal load under the real working conditions. By observing the PCM state in Fig. 5 (b), the smaller amount of PCM in 10% PS converts faster from solid to liquid than that in 30% PS. Compared with the reference case of grout screw pile back-filling, using 30% PS as the filler results in lower fluid temperature in the first 24 h and then stays at a similar value in the remaining 24 h. Since the $\lambda_{eff}$ of 30% PS is similar to that of the grout as shown in Table 2, keeping PCM at the transition stage to absorb (more) heat makes the energy screw have a smaller operating fluid temperature than back-filling with other materials with similar $\lambda_{eff}$. In other words, selecting a proper $T_{pc}$ for PCM is critical since it controls the PCM state under the same heating/cooling load.

Fig. 5(a) also shows that the mean fluid temperature in 30% PC is lower than that in the system using 10% PS in the first 6 h but becomes higher later, especially when the PCM is completely converted to liquid after the 18th hour. This observation indicates the importance of incorporating solids with high thermal conductivity again rather than only focusing solely on the amount of PCM.

As the thermal conductivity of water is twenty times larger than that of air, saturating the pile filler can increase its $\lambda_{eff}$ substantially. Fig. 6 compares the resulting mean fluid temperature of selected "dry" and "saturated" PCM-sand mixtures cases with a $T_{pc}$ of 25 °C and their associated PCM state for 48 h of continuous heat rejection to the ground. The real-time mean fluid temperature in Fig. 6(a) shows that a saturated condition can always lead to a lower fluid temperature than a dry

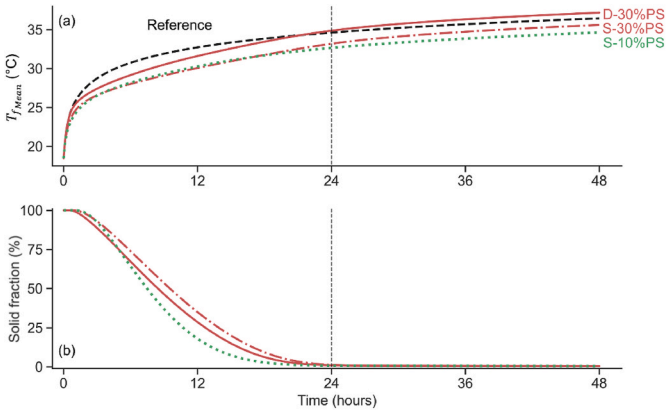


**Fig. 6.** The comparison between using dry and saturated PCM-sand mixtures with a $T_{pc}$ of 25 °C on the mean fluid temperature (a) and their associated PCM state under 48 h of heating.

condition, by comparing dry 30%PS (D-30%PS) with its saturated counterpart S–30%PS. Furthermore, a smaller amount of PCM added to saturated sand (S–10%PS) leads to an even lower temperature. Fig. 6(b) presents that the saturated S–30%PS melts later than its dry counterpart D-30%PS. In addition, less PCM content in S–10%PS also leads to a slightly delayed phase change process start than S–30%PS, but completes the phase transition earlier since water has a larger thermal conductivity than PCM, and lower PCM content means that less latent heat is needed to complete the phase change.

Considering all the variations in parameters tested in the numerical simulations, observations are summarised in Fig. 7 With taking the energy screw pipe filled by grout as a reference, a measure to indicate the performance of PCM energy screw piles ($\Delta\overline{T}_{ref-PCM}$) is herein defined as the difference of 48 h-averages of the mean fluid temperature between using grout ($T_{f_{MeanRef}}$) and PCM-sand mixture ($T_{f_{MeanPCM}}$) (see Appendix II for details).

$$\Delta\overline{T}_{ref-PCM} = Average_{48hrs}\left(T_{f_{MeanRef}}\right) - Average_{48hrs}\left(T_{f_{MeanPCM}}\right)$$

Fig. 7 shows this measure $\Delta\overline{T}_{ref-PCM}$ calculated under the two different mixtures moisture conditions (i.e., dry and saturated). For simplicity and ease of comparison, the ground thermal properties were kept constant as per Table 1. While the fluid temperature difference of

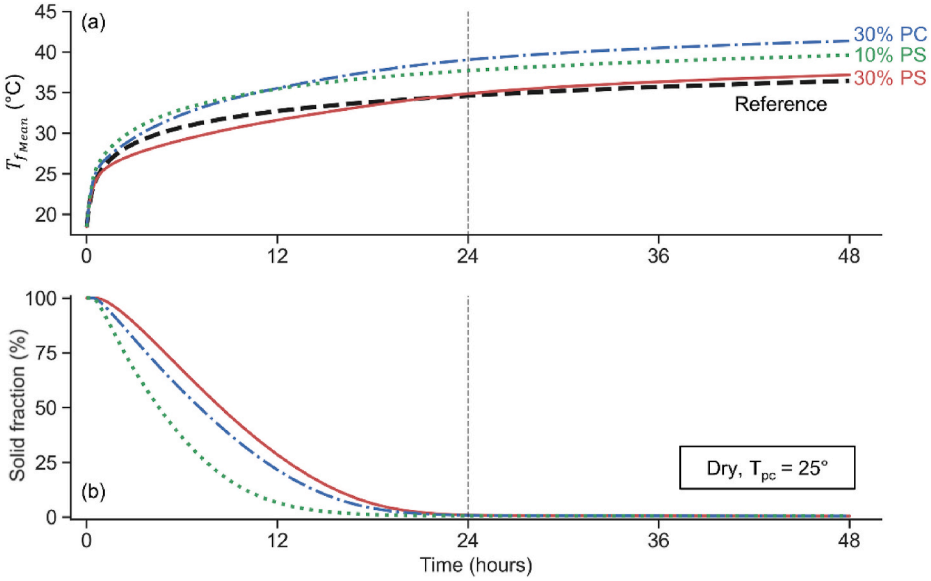


**Fig. 5.** The resulting mean fluid temperature (a) and associated PCM state under 48 h of heating when using three dry PCM-solid mixtures with a $T_{pc}$ of 25 °C.

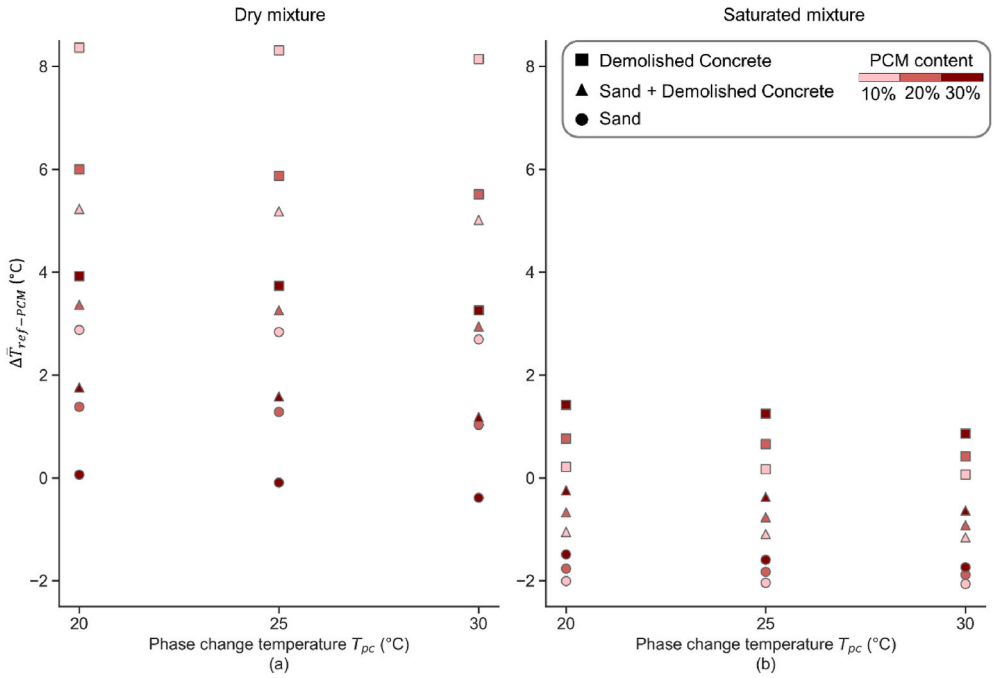


**Fig. 7.** The fluid temperature difference using PCM-sand mixtures compared with using grout as pile backfill under a constant heating rejection to the ground (i.e., cooling a building): (a) dry mixtures and (b) saturated mixtures.

0 °C indicates the reference itself using grout as the back-filling material (conventional grout used), fluid temperature difference below 0 °C means that the PCM-sand mixture absorbs more heat than grout under the consistent heating rejection to the ground, thus indicating to better performance when cooling a building.

Fig. 7 (a) shows that, in general, increasing the PCM fraction tends to decrease mean fluid temperature. However, efficiency gains with respect to the reference case are only significant when in saturated conditions. There are only two cases when efficiencies are marginally gained under dry conditions: the 30% PCM-sand mixtures for $T_{pc}$ of 25 and 30 °C for the cases tested. The 30% PCM-sand mixture in dry conditions has a lower fluid temperature than using the grout in the traditional system. However, changing sand to demolished concrete to be mixed with the same 30% PCM leads to an undesired higher fluid temperature (leading to a worse GSHP system COP). These results indicate the importance of the thermal conductivity of the solid to mix the PCM within the efficiency of the new system since recycled concrete presents a much lower thermal conductivity than quartz sand (3.12 and 7.70 W/m·K, respectively) even though the heat capacity of concrete is larger (1060 and 740 J/(kg·K), respectively). The high thermal conductivity of solid can enhance the rate of charging and discharging heat of the PCM-solid mixtures [51].

Fig. 7 (b) shows that most PCM energy screw piles using the most saturated mixtures have lower fluid temperatures than the reference case, i.e., better GSHP system performance. Furthermore, while a larger fraction of PCM corresponds to a lower fluid temperature when PCM-solid mixtures are dry, a smaller fraction of PCM is preferred to achieve a lower fluid temperature when PCM-solid mixtures are saturated (i.e., an opposing trend). This tendency may be because water has a larger thermal conductivity than PCM, with 0.6 and 0.36 W/m·K, respectively. Consequently, the usage of PCM can be reduced when backfilling is saturated, 10% PCM mixed with sand can yield a significant 2.6 °C lower fluid temperature than using grout as pile backfill.

### 3.1.2. Phase change temperature

For dry mixtures, Fig. 7 (a) showed that the increase of $T_{pc}$ can decrease the fluid temperature in water pipes. To investigate the effect of $T_{pc}$ on the efficiency of the new energy screw piles, the real-time fluid temperature and PCM state in 30% PS are presented in Fig. 8. PCM with a lower $T_{pc}$ leads to a lower fluid temperature soon after turning the heat pump on but a higher fluid temperature at the end of 48-h constant heating rejection to the ground. The lower fluid temperature when using PCM with a $T_{pc}$ of 20 °C in the first 5 h is because the solid PCM is melted into liquid earlier as shown in Fig. 8(b). Even though the phase transformation is fully completed at the 6th hour in Fig. 8(b), the incorporation of PCM can still result in a lower fluid temperature than using grout up until the 11th hour (Fig. 8(a)). At the same moment, adopting PCM with a $T_{pc}$ of 30 °C compels the PCM to stay partially solid with untapped potential to store more heat. Hence, the associated fluid temperature in Fig. 8(a) is lower than that of the reference case for up to 46 h of continuous operation. The observations imply that the $T_{pc}$ determines the process of latent heat storage/release when under the same thermal load, with lower $T_{pc}$ resulting in a faster process while high $T_{pc}$ resulting in a slower process. With more PCM having $T_{pc}$ of 30 °C melted, the associated real-time mean fluid temperature is lower than the case selecting the $T_{pc}$ of 20 °C after the 8th hour and lower than the case adopting the $T_{pc}$ of 25 °C after the 15th hour. The latent heat of the PCM with the $T_{pc}$ of 30 °C has not been fully consumed in 48 h, compared with PCMs in the other two cases are changed to liquid in an early stage. PCM in solid state has a larger thermal conductivity than in liquid state, so staying in solid state for a longer time allows a quicker heat exchange between the water pipe and the ground. The advantage is more obvious when using a larger amount of PCM. It can be observed from Fig. 7 (a) that changing the $T_{pc}$ from 20 to 30 °C for 30% PS results in a larger fluid temperature change than using 10% PS.

### 3.1.3. Thermal radius

Since screw piles have a small diameter and relatively low bearing capacity, a higher density of screw piles is typically required to sustain the same structural load compared with traditional energy piles with larger diameters. In some cases, screw piles are closely spaced and their centre-to-centre spacing can be less than three times the pile diameter (0.342 m) [52]. As a result, the small pile spacing might cause thermal interference if a large amount of PCM energy screw piles is expected to be used. The pile spacing of 0.342 m was considered in this study since only two days period was simulated and the ground temperature could

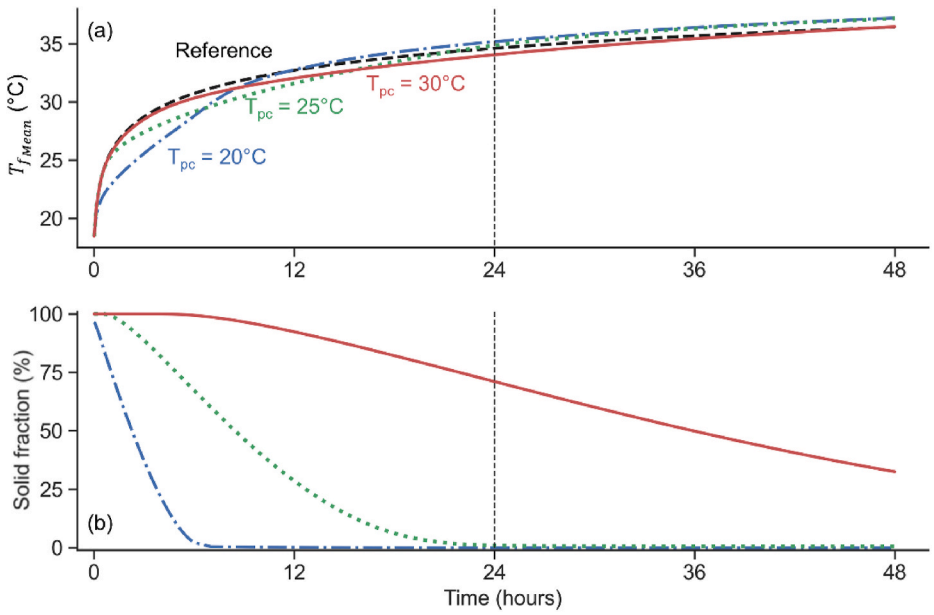


**Fig. 8.** Average fluid temperature (a) and remained solid PCM (b) under constant heating rejection to the ground using sand-30% PCM mixture.

be accumulated (i,e., thermal radius increases) over the lifespan of the energy piles and the building. Fig. 9 shows the temperature distributions from the pile centre to half of the pile spacing (i.e., 0.171 m) along the central line between inlet and outlet (line OA in Fig. 2), at the depth of 6.5 m for the various mixtures. Short names were given for the five mixtures in a format of X-XX%PY-TZZ. The first X is either D or S to represent a dry or saturated condition. XX%P indicates the PCM fraction in the mixture. The Y after P indicates the solid material in the mixture, quartz sand is used if Y is S while demolished concrete is used if Y is C. ZZ after T presents the $T_{pc}$ of the PCM. Fig. 9 exhibits that the utilisation of D-30%PS-T25 as pile backfill results in the lowest temperature and thus smallest thermal radius at the 6th and the 12th hour. In contrast, D-30% PC-T30 leads to the smallest thermal radius at the 24th and 48th hour even though its corresponding temperature at the pile centre is always the highest at different times.

The temperature distribution between D-30%PS-T25 and D-30%PS-

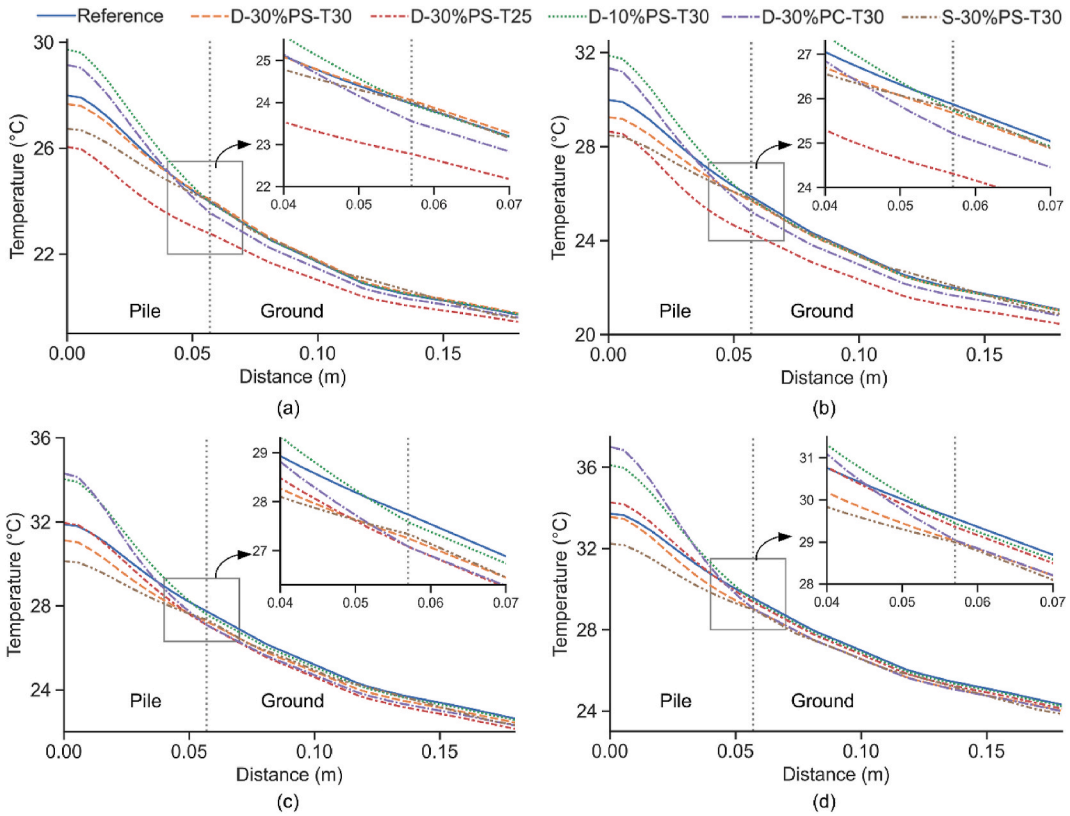


**Fig. 9.** Thermal radii result from different mixtures at the 6th hour (a), 12th hour (b), 24th hour (c) and 48th hour (d). The vertical dash line indicates the pile outer wall.

T30 is compared to investigate the effect of $T_{pc}$ on the thermal radius. Fig. 9 presents that the lower $T_{pc}$, the lower temperature both inside and outside the pile in the first 12 h, which is attributed to the early phase-change transition in D-30%PS-T25, as shown in Fig. 10 (a) and (b). At the 24th hour, the solid PCM in D-30%PS-T25 is almost fully transformed to liquid and has negligible capacity to absorb more heat. Hence, the temperature inside the pile is higher than that by adopting D-30%PS-T30. The full consumption of latent heat in PCM also results in more heat being transferred to the ground. Hence, the temperature outside the pile experiences a large increase from the 12th hour to the 24th hour. It reaches a similar value to the case using D-30%PS-T30 at the 24th hour. Although a higher $T_{pc}$ results in a smaller thermal radius in a long term under constant heating, the realistic thermal load is intermittent, and less than 12 h of heating might be required each day and thus a lower $T_{pc}$ might be a better selection. Hence, the observation also hints that the selection of $T_{pc}$ should comply with the thermal load of the buildings to satisfy.

Reducing the amount of PCM in D-30%PS-T30 from 30% to 10% (i.e., D-10%PS-T30) and replacing sand with demolished concrete (i.e., D-30%PC-T30) results in a similar $\lambda_{eff}$ (1.1 and 1.0 W/m K when PCM at solid state, respectively) but distinct specific heat capacity (808.5 and 1230.0 J/kg K, respectively). Fig. 9 shows that screw piles using these two mixtures always have a much higher temperature inside piles than that using D-30%PS-T30. The PCM state in the piles using these two mixtures are also similar, as shown in Fig. 10 (c) and (d). Therefore, it can be concluded that the $\lambda_{eff}$ of the pile backfill plays a key role in the PCM state and the temperature inside piles. It is also observed that the smaller $\lambda_{eff}$ of these two mixtures than that of D-30%PC-T30 results in an earlier phase change under the same $T_{pc}$. Although D-10%PS-T30 and D-30%PC-T30 have a synchronous phase change, the smaller specific heat capacity and latent heat of D-10%PS-T30 can only store a limited amount of heat and thus more heat is transferred to the ground, resulting in a higher ground temperature.

Turning D-30%PS-T30 from dry condition to saturated enables the mixture to have a higher $\lambda_{eff}$. Fig. 10 (e) shows that the superior $\lambda_{eff}$ allows the PCM in S–30%PS-T30 to melt slower than its dry peer shown in Fig. 10 (a). The high $\lambda_{eff}$ and specific heat capacity also make the temperature inside the pile the lowest under the same $T_{pc}$. However, its associated temperature outside the pile is higher than that of D-30%PC-T30 at the 24th hour due to the late phase transaction in S–30%PS-T30.

### 3.2. Intermittent heating injection to the ground

The realistic operating environment of a heat pump can be complex since ambient temperature and working hours vary. The ground source heat pump might be turned on and off several times in a single day, which introduces thermal load peaks. This working condition was simulated in this section by applying the same 0.65 kW building cooling power but only for 12 h per day for a week to the PCM energy screw piles with various backfills. PCMs with different $T_{pc}$ were also included to investigate the effect of applying PCM in a screw pile on daily temperature peaks.

The intermittent cooling of the soil represents the GHE thermal recovery effect when the GSHP is off. Same as the observation from Figs. 8 and 11 shows that the fluid temperature using PCM with $T_{pc}$ of 20 °C is the lowest in the first 6 h, but soon becomes higher than the cases using

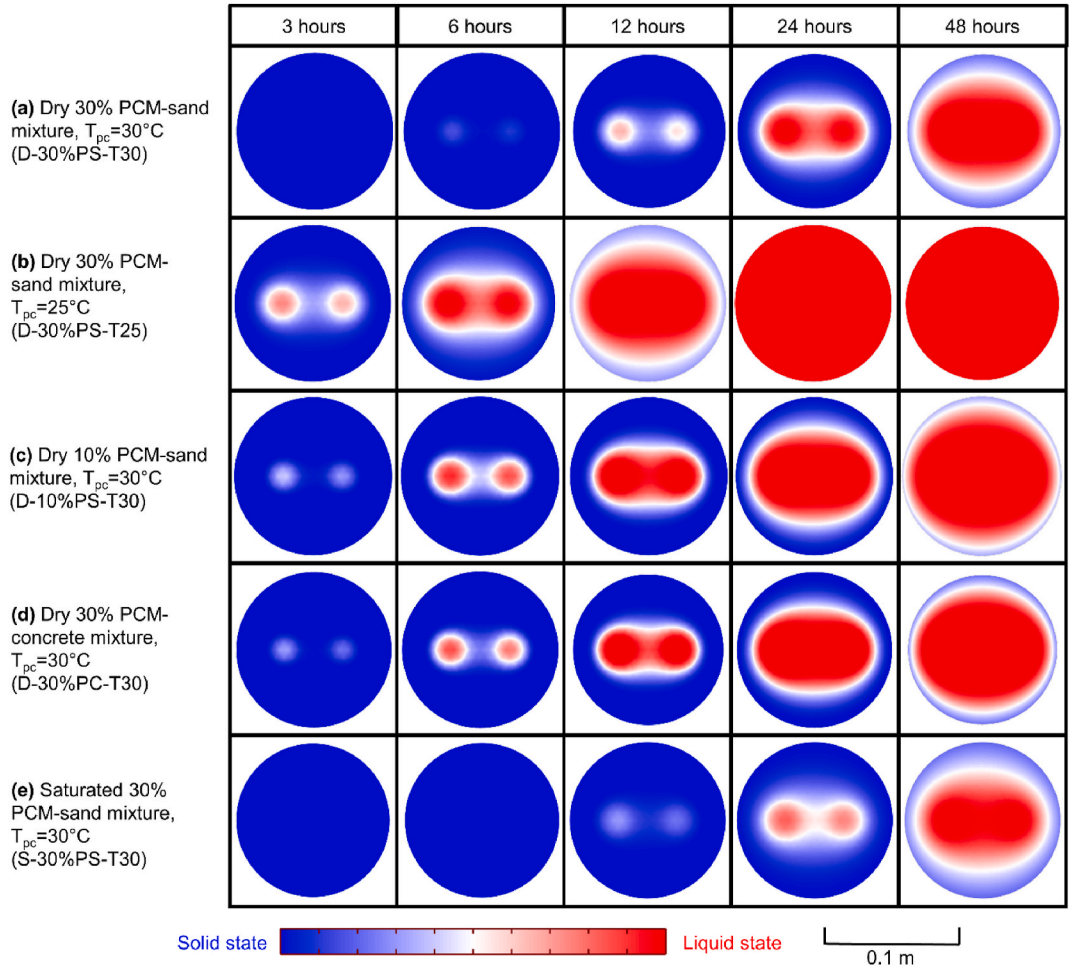


**Fig. 10.** PCM state during GSHP operation.

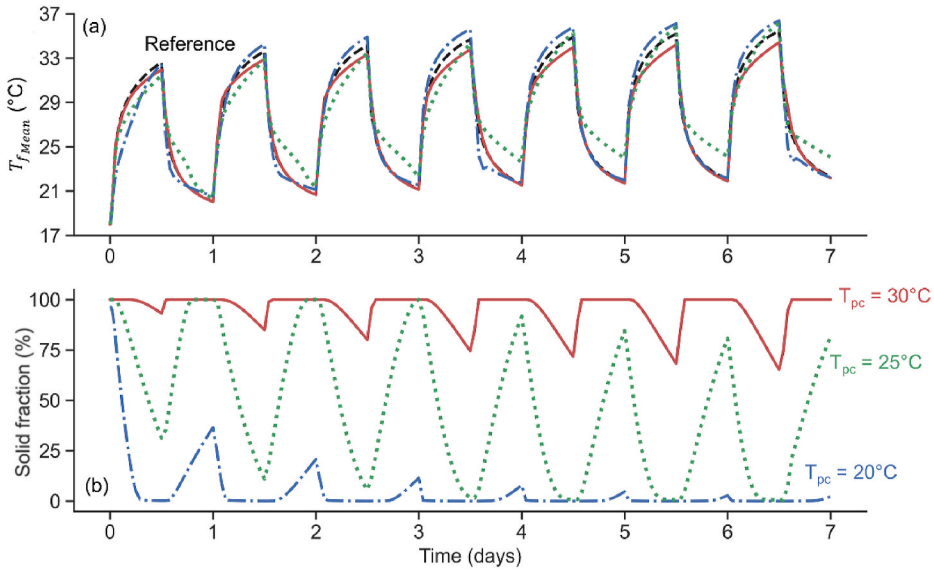


**Fig. 11.** Average fluid temperature (a) and remained solid PCM (b) under intermittent heating injection to the ground using dry sand-30% PCM mixture of various melting temperatures $T_{pc}$.

PCM with $T_{pc}$ of 25 and 30 °C. After 12 h, the system using PCM with $T_{pc}$ of 25 °C has transformed around 70% of solid PCM to liquid and resulted in the lowest peak while only 7% of solid PCM with $T_{pc}$ of 30 °C has been transformed. As the heat is dissipated passively in the second half-day, the fluid temperature at the end of the day cannot be recovered to the original level. The accumulated heat melts more solid PCM in the following days. On the fourth day at noon, all the PCM with $T_{pc}$ of 25 °C is transformed to liquid while around 30% of PCM with $T_{pc}$ of 30 °C is melted, resulting in PCM with $T_{pc}$ of 30 °C having the lowest temperature peak. The demonstration reinforced the importance of avoiding consuming all the latent heat during the system operation.

Fig. 12 (a) displays the PCM state in the pile at different times. The PCM is melted more on the 6.5th day than that on the 1.5th day due to the accumulated heat. In addition, more PCM is transformed from solid to liquid along the x-direction than in the y-direction since the inlet and outlet pipes are lined up along the x-direction. The temperature profile of the energy screw pile on the 6.5th day is shown in Fig. 12 (b). Since the PCM with $T_{pc}$ of 30 °C is used in this simulation, the 30 °C temperature contour matches the boundary between solid and liquid PCM. An oval shape of the liquid PCM can be observed in Fig. 12 (b).

Section 3.1 has demonstrated that a smaller thermal radius can be achieved by using PCM-solid mixtures than using grout under constant heating rejection to the ground. Compared with the thermal radius reduction under a constant rejection load at the end of the 2nd day in Figs. 9(d), Fig. 13 (a) presents that the thermal radius using D-30%PC-T30 and D-30%PS-T30 can reduce more on the 2.5th day under an intermittent load. The reduction could be more obvious on the 6.5th day, as shown in Fig. 13 (b). It is also worth noticing that D-30%PS-T25 results in the smallest thermal radius at the 2.5th day under intermittent heating by a significant margin while it does not reduce the thermal radius much under constant heating. This is because its PCM was fully converted to liquid way before the end of the second day under constant heating while the PCM can be discharged under intermittent heating, so here by the 2.5th the D-30%PS-T25 mixture still using available latent heat. However, the thermal radius reduction using D-30%PS-T25 on the 6.5th day is not the smallest since the PCM has been fully transformed to liquid early.

To evaluate the general performance of incorporating PCM in reducing the daily temperature peaks, the average of the seven peaks in the week was calculated and its difference between using PCM in a screw pile and the reference using grout is selected as an index (see Appendix II for details). Fig. 14 indicates that incorporating PCM with $T_{pc}$ of 30 °C has the lowest average fluid temperature peak when mixing with the same solid particles. In addition, incorporating a higher content of PCM

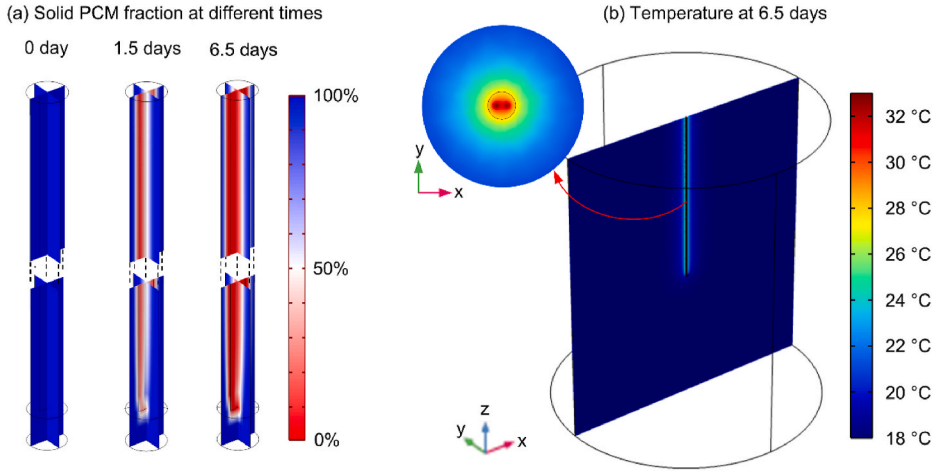


**Fig. 12.** PCM phase transition state (a) and temperature distribution on the 6.5th day of operation (b). $T_{pc}$ is 30 °C.

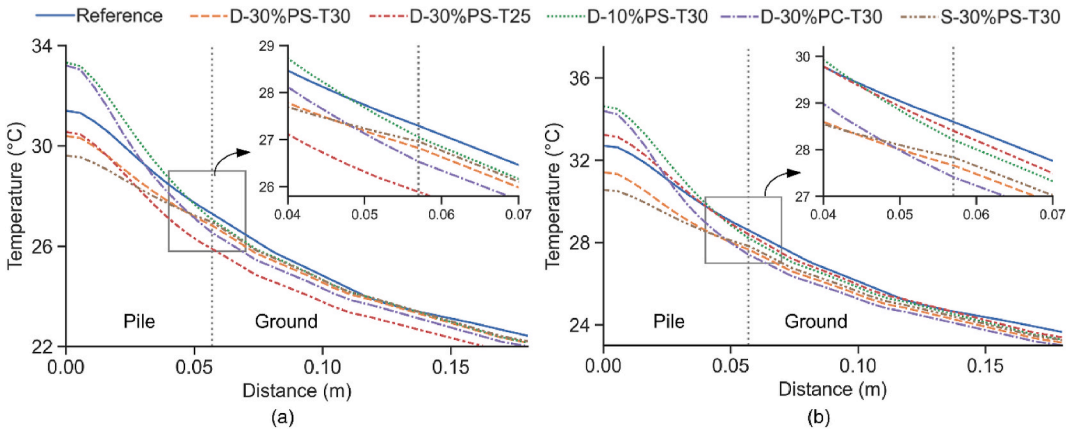


**Fig. 13.** Thermal radii of systems with different mixtures 2.5th day (a) and 6.5th day (b) of operation.

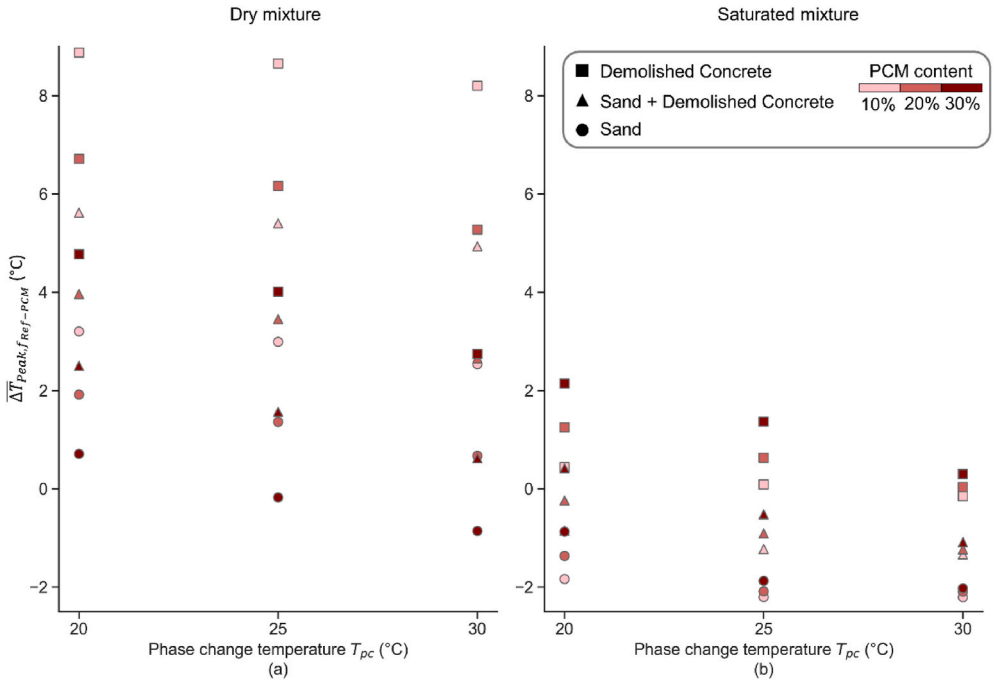


**Fig. 14.** The response of various mixtures to the average peak fluid temperature difference compared to the reference case using grout: (a) dry mixtures and (b) saturated mixtures.

in dry mixtures while a lower content of PCM in a saturated mixture is beneficial to achieving a lower temperature peak. For the saturated mixtures with $T_{pc}$ of 30 °C, the effect of the PCM percentage in the peak temperature value is barely noticeable.

### 3.3. Realistic thermal load

After using simple thermal loads to investigate the impacts of materials properties on the performance of PCM-enhanced energy screw pile, a thermal load from a real project of a large educational building in Melbourne, Australia was used for further studying the realistic

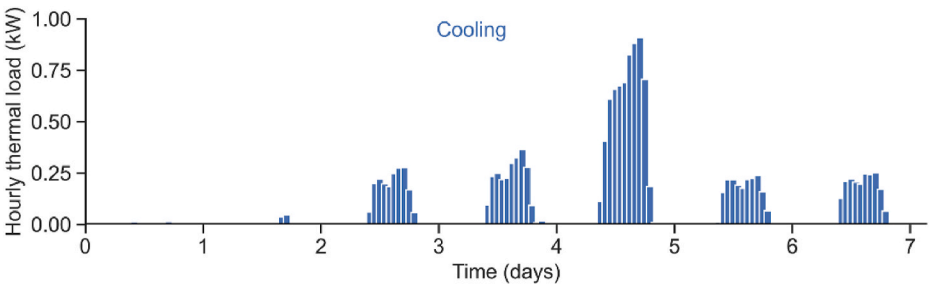


**Fig. 15.** The realistic thermal load of a single energy pile for an educational building in the warmest week in Melbourne, Australia.

performance of the proposed system. Fig. 15 presents the hourly cooling thermal load of a single pile in the warmest week from the design. Since the GSHP cools down the building by injecting the heat coming from it into the ground, low fluid and ground temperatures are desired. The real thermal load increases in the first four days following a big climb to reach its crest on the fifth day, and then drops to a low level in the last two days.

Since the heat pump operates intermittently and the daily thermal load varies in the week, the average fluid temperature was calculated by only considering the moments when the heat pump was on. Its difference between using PCM-solid mixtures and using grout was presented in Fig. 16. Similar to the previous results under constant and intermittent building cooling loads, a higher PCM fraction leads to a lower fluid temperature in dry mixtures while a higher fluid temperature in saturated mixtures, when utilising the proposed system under a real thermal load. However, the $T_{pc}$ shows a distinct impact on the fluid temperature, with PCM having lower $T_{pc}$ resulting in a larger temperature reduction.

By observing the real-time temperature variation and PCM state in Fig. 17, it is found that the system using PCM with $T_{pc}$ of 20 °C has the lowest daily peak except for the fifth day, because the state of PCM with $T_{pc}$ of 20 °C changes in six days while PCM with $T_{pc}$ of 25 °C and 30 °C experiences little phase change. In other words, PCM with $T_{pc}$ of 20 °C has a high *utilisation ratio*. On the fifth day, the large thermal load turns PCM with $T_{pc}$ of 20 °C into liquid completely while PCM with $T_{pc}$ of 25 and 30 °C partially. The consumption of the latent heat from around 75% PCM with $T_{pc}$ of 25 °C results in the associated lowest peak on the day. This investigation implies that consuming more latent heat of PCM when it is in the transient phase (both solid and liquid) benefits the average performance of the proposed system. If using PCM only for an emergency purpose such as reducing the temperature on an extremely hot day, a PCM with a higher $T_{pc}$ that changes its phase substantially only on the day is a better choice.

Fig. 18 (a) shows that all the energy screw piles with PCM have lower temperatures outside the pile than using grout on the 4.75th day. D-30% PS-T25 has the lowest temperature outside the pile since its PCM is still in transition. By contrast, the PCM in D-30%PS-T20 has finished phase change, resulting in a larger thermal radius. On the 6.75th day, only PCM in D-30%PS-T20 has phase transition, so its associated thermal radius is the smallest. Fig. 18 (b) presents that using a higher $T_{pc}$ such as D-30%PS-T25 and D-30%PS-T30 can reduce the temperature inside the pile due to their larger $\lambda_{eff}$. However, their associated temperature outside the pile is larger than that using grout. Hence, over-enhancing $\lambda_{eff}$ of PCM-solid mixtures might deteriorate the thermal interference between energy piles.

## 4. Conclusions

A new concept of energy screw pile coupled with PCM was introduced in this work. To study the performance of the new pile, the associated GSHP system was numerically simulated, considering various PCM-solid mixtures, moisture conditions, phase change temperature of PCM, and ground heating injection schedules. By employing the conventional screw pile filled with grout as a reference, results show that the proposed PCM energy screw pile can reduce the fluid temperature in the heat exchanger and the thermal interference with a suitable selection of PCM-solid mixture.

The $\lambda_{eff}$ of the PCM-solid mixture dictates the phase change, with higher $\lambda_{eff}$ slowing down the transition and resulting in a lower fluid temperature, thus increasing COP in the building cooling mode of operation (heat rejection to the ground). In addition, a larger PCM fraction in the dry mixtures can absorb more heat and reduce the fluid temperature. As water has larger thermal conductivity and specific heat capacity than air and PCM, a wet moisture condition with lower PCM usage can also achieve a satisfying low fluid temperature.

Phase change temperature $T_{pc}$ is a key property when selecting PCM and its selection depends on the operation schedule and purpose. Under a constant rejection of heat to the ground, a high $T_{pc}$ that delays the PCM transition and keeps the PCM at solid state for a long time is preferred since solid PCM has larger thermal conductivity than at liquid state. Under an intermittent or real heat rejection, allowing PCM to be recovered and keeping PCM at transient state with a high utilisation ratio is recommended. Generally, a $T_{pc}$ corresponding with the high utilisation ratio is desired when aiming to achieve an average lower fluid temperature during the long-term operation. In contrast, a higher $T_{pc}$ is better for an emergency to reduce the fluid temperature on an extremely hot day.

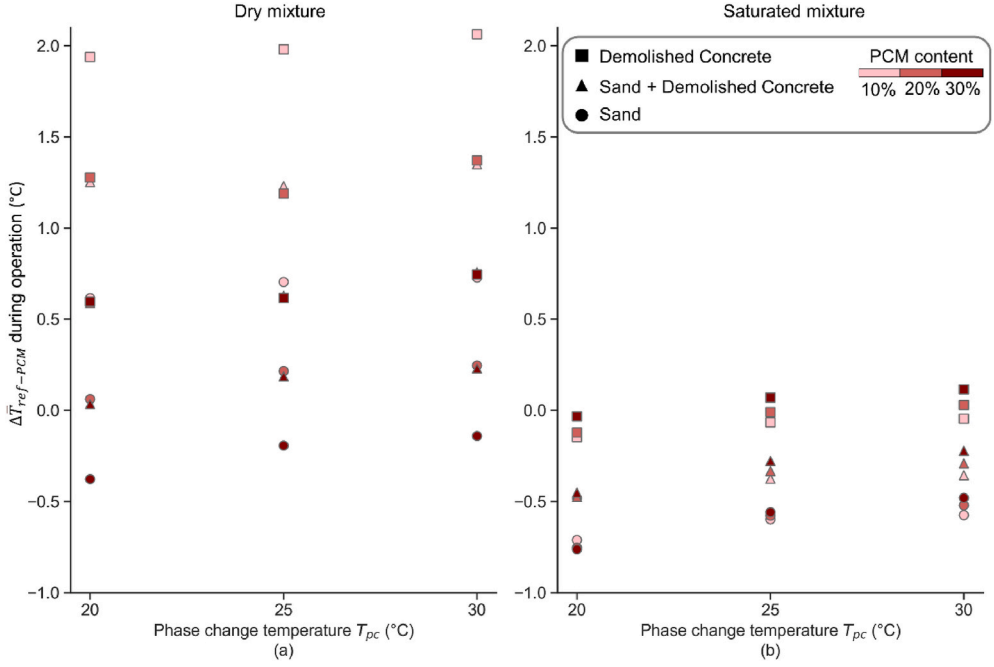


**Fig. 16.** The response of various mixtures to the average fluid temperature difference compared to the reference case using grout in the screw piles under a real building thermal load in summer (a) dry mixtures and (b) saturated mixtures.

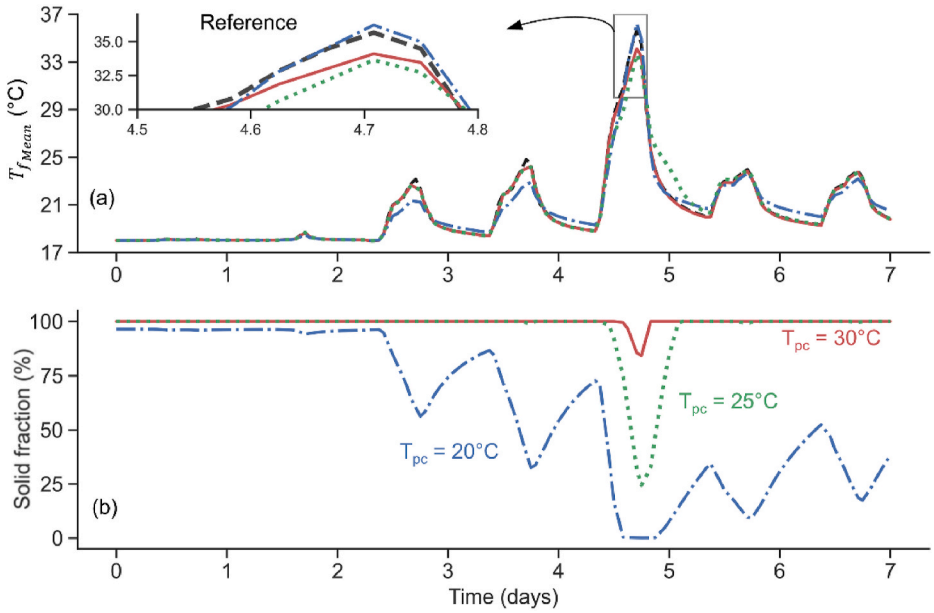


**Fig. 17.** Average fluid temperature(a) and remained solid PCM (b) under realistic heating injection using dry sand-30% PCM mixture.

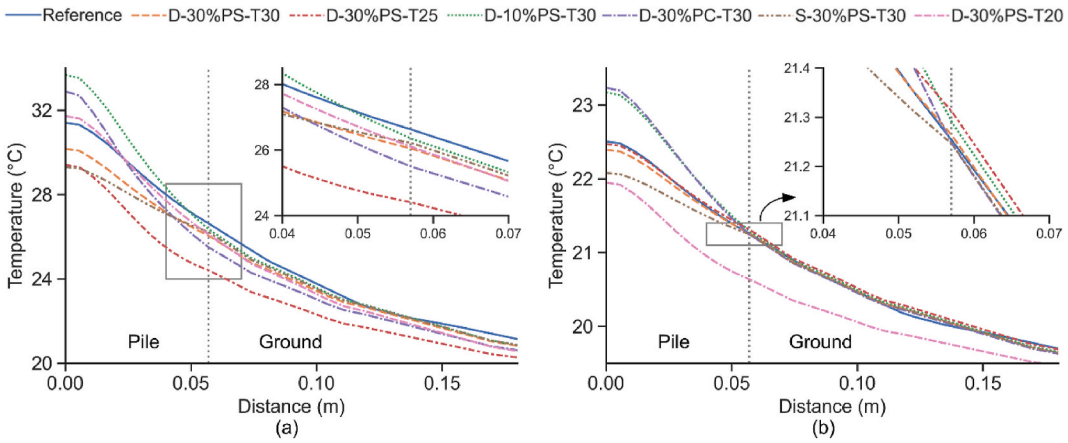


**Fig. 18.** Thermal radii of systems with different mixtures at 4.75th day (a) and 6.75th day (b).

Screw piles have lower bearing capacity than traditional piles with large diameters, so smaller pile spacing and the associated increased thermal interference should be considered. Pile backfills with larger specific heat capacity can store more heat inside the pile, a smaller amount of heat transferred to the ground can reduce the thermal radius. While larger $\lambda_{eff}$ of pile backfill can reduce the temperature inside the pile, it might enhance the heat transfer into the ground and deteriorate the thermal interference between energy screw piles.

To better understand the thermal behaviour of the new PCM-based energy screw pile, full-scale field tests using a saturated sand-PCM mixture and normal grout filling will be conducted in the future. The fluid temperatures at the inlet and outlet of the two systems will be monitored to compare their efficiency. The temperatures of backfilling and ground surrounding the piles at different depths will be recorded to compare their extent of thermal interference.

## Author Statement

**Wenbin Fei:** Conceptualization, Methodology, Investigation, Software, Formal analysis, Writing – original draft, Visualization, Funding acquisition., **Luis A. Bandeira Neto:** Methodology, Investigation, Software, Formal analysis, Writing – original draft, Visualization, **Sheng Dai:** Resources, Formal analysis, Writing – review & editing., **Douglas D. Cortes:** Resources, Investigation, Writing – review & editing., **Guillermo A. Narsilio:** Formal analysis, Writing – review & editing, Funding acquisition.

## Declaration of competing interest

The authors declare that they have no known competing financial interests or personal relationships that could have appeared to influence the work reported in this paper.

## Acknowledgments

The authors acknowledge the Early Career Research Grant (2022ECR085) provided by the University of Melbourne and the Linkage Project (LP160101486) provided by the Australian Research Council. This research was supported by the use of the Nectar Research Cloud, a collaborative Australian research platform supported by the NCRIS-funded Australian Research Data Commons (ARDC).

## Appendix I. Properties of PCM-solid mixtures

| Sand | Moisture | PCM content | Density $\rho$ (kg/m$^3$) | Effective thermal conductivity $\lambda_{eff}$ (W/m K) | Specific heat capacity $C_p$ (J/kg K) | Latent Heat $LH$ (kJ/kg) |
|---|---|---|---|---|---|---|
| Quartz sand | Dry | 10% | 1667 (s) | 1.1 (s) | 808.5 (s) | 11.3 |
| | | | 1667 (l) | 1.0 (l) | 808.5 (l) | |
| | | 20% | 1744 (s) | 1.4 (s) | 871 (s) | 21.5 |
| | | | 1744 (l) | 1.2 (l) | 871 (l) | |
| | | 30% | 1821 (s) | 1.8 (s) | 928.2 (s) | 30.9 |
| | | | 1821 (l) | 1.4 (l) | 928.2 (l) | |
| | Saturated | 10% | 1967 (s) | 2.6 (s) | 1324.5 (s) | 9.5 |
| | | | 1967 (l) | 2.4 (l) | 1324.5 (l) | |
| | | 20% | 1944 (s) | 2.5 (s) | 1212.6 (s) | 19.3 |
| | | | 1944 (l) | 2.1 (l) | 1212.6 (l) | |
| | | 30% | 1921 (s) | 2.4 (s) | 1098.1 (s) | 29.3 |
| | | | 1921 (l) | 1.8 (l) | 1098.1 (l) | |
| Demolished Concrete | Dry | 10% | 1427 (s) | 0.6 (s) | 1122.8 (s) | 13.2 |
| | | | 1427 (l) | 0.6 (l) | 1122.8 (l) | |
| | | 20% | 1504 (s) | 0.8 (s) | 1179.1 (s) | 25.0 |
| | | | 1504 (l) | 0.7 (l) | 1179.1 (l) | |
| | | 30% | 1581 (s) | 1.0 (s) | 1230 (s) | 35.6 |
| | | | 1581 (l) | 0.8 (l) | 1230 (l) | |
| | Saturated | 10% | 1727 (s) | 1.5 (s) | 1655.9 (s) | 10.9 |
| | | | 1727 (l) | 1.4 (l) | 1655.9 (l) | |
| | | 20% | 1704 (s) | 1.5 (s) | 1532.7 (s) | 22.0 |
| | | | 1704 (l) | 1.2 (l) | 1532.7 (l) | |
| | | 30% | 1681 (s) | 1.4 (s) | 1406.1 (s) | 33.5 |
| | | | 1681 (l) | 1.1 (l) | 1406.1 (l) | |
| Quartz sand + demolished concrete | Dry | 10% | 1547 (s) | 0.8 (s) | 953.5 (s) | 12.1 |
| | | | 1547 (l) | 0.7 (l) | 953.5 (l) | |
| | | 20% | 1624 (s) | 1.0 (s) | 1013.7 (s) | 23.1 |
| | | | 1624 (l) | 0.9 (l) | 1013.7 (l) | |
| | | 30% | 1701 (s) | 1.3 (s) | 1068.4 (s) | 33.1 |
| | | | 1701 (l) | 1.0 (l) | 1068.4 (l) | |
| | Saturated | 10% | 1847 (s) | 2.0 (s) | 1479.5 (s) | 10.2 |
| | | | 1847 (l) | 1.8 (l) | 1479.5 (l) | |
| | | 20% | 1824 (s) | 1.9 (s) | 1362.1 (s) | 20.6 |
| | | | 1824 (l) | 1.6 (l) | 1362.1 (l) | |
| | | 30% | 1801 (s) | 1.8 (s) | 1241.9 (s) | 31.3 |
| | | | 1801 (l) | 1.4 (l) | 1241.9 (l) | |

Note: s stands for solid state while l stands for liquid state.

## Appendix II. Definition of $\Delta\overline{T}_{f_{Ref-PCM}}$ and $\overline{\Delta T}_{Peak f_{Ref-PCM}}$

This appendix presents the parameters used for the comparison between the performance of new PCM-screw piles presented in this work and a reference case using a concrete filled screw pile. The $\Delta\overline{T}_{f_{Ref-PCM}}$ presented in Figs. 7 and 16 is the average fluid temperature difference while $\overline{\Delta T}_{Peak f_{Ref-PCM}}$ shown in Fig. 14 is the average peak fluid temperature difference. Their definitions are illustrated in Fig AII - 1 and Fig AII - 2, respectively.

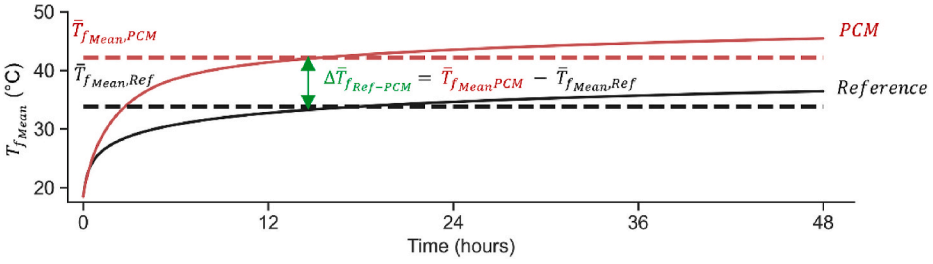


**Fig. AII - 1.** Definition of the difference of the mean fluid temperatures over the period registered by the use of the PCM-sand mixture of interest as filling and the reference case (grout filling).

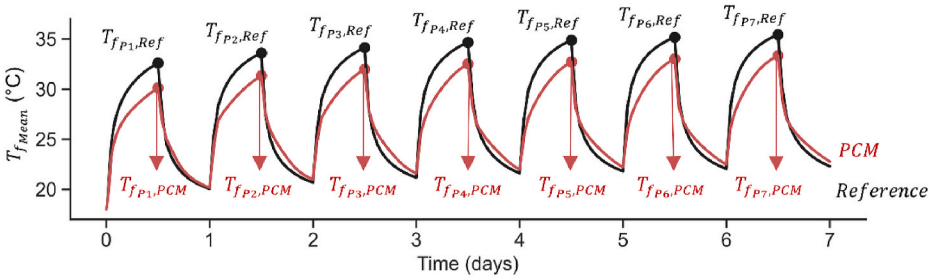


$$\overline{\Delta T}_{Peak,f_{Ref-PCM}} = \frac{\sum_{i=1}^{7}\left(T_{f_{Pi},PCM} - T_{f_{Pi},Ref}\right)}{7}$$

**Fig. AII - 2.** Definition of the average difference of daily peak fluid temperatures registered by the use of the PCM-sand mixture of interest as filling and the reference case (grout filling).

## References


[1] S. Bouckaert, A.F. Pales, C. McGlade, U. Remme, B. Wanner, L. Varro, D. D'Ambrosio, T. Spencer, Net Zero by 2050: A Roadmap for the Global Energy Sector, 2021.

[2] R.A. Beier, Transient heat transfer in a U-tube borehole heat exchanger, Appl. Therm. Eng. 62 (1) (2014) 256–266, https://doi.org/10.1016/j.applthermaleng.2013.09.014.

[3] Rao Martand Singh, Abubakar Kawuwa Sani, Tony Amis, in: Trevor M. Letcher (Ed.), 15 - An overview of ground-source heat pump technology, Managing Global Warming, Academic Press, 2019, pp. 455–485, https://doi.org/10.1016/B978-0-12-814104-5.00015-6. ISBN 9780128141045.

[4] Q. Lu, G.A. Narsilio, Cost effectiveness of energy piles in residential dwellings in Australia, Curr. Trends Civ. Struct 3 (3) (2019) 1–6, https://doi.org/10.33552/CTCSE.2019.03.000564.

[5] N. Makasis, G.A. Narsilio, Energy diaphragm wall thermal design: the effects of pipe configuration and spacing, Renew. Energy 154 (2020) 476–487, https://doi.org/10.1016/j.renene.2020.02.112.

[6] A. Bidarmaghz, N. Makasis, W. Fei, G.A. Narsilio, An efficient and sustainable approach for cooling underground substations, Tunn. Undergr. Space Technol. 113 (2021), 103986, https://doi.org/10.1016/j.tust.2021.103986.

[7] X. Bao, X. Qi, H. Cui, W. Tang, X. Chen, Experimental study on thermal response of a PCM energy pile in unsaturated clay, Renew. Energy 185 (2022) 790–803, https://doi.org/10.1016/j.renene.2021.12.062.

[8] P. Hu, J. Zha, F. Lei, N. Zhu, T. Wu, A composite cylindrical model and its application in analysis of thermal response and performance for energy pile, Energy Build. 84 (2014) 324–332, https://doi.org/10.1016/j.enbuild.2014.07.046.

[9] J. Sarkar, S. Bhattacharyya, Application of graphene and graphene-based materials in clean energy-related devices Minghui, Arch. Therm. 33 (4) (2012) 23–40, https://doi.org/10.1002/er.1598.

[10] M. Bottarelli, M. Bortoloni, Y. Su, C. Yousif, A.A. Aydın, A.J.A.T.E. Georgiev, Numerical analysis of a novel ground heat exchanger coupled with phase change materials, Appl. Therm. Eng. 88 (2015) 369–375, https://doi.org/10.1016/j.applthermaleng.2014.10.016.

[11] L. Xu, L. Pu, S. Zhang, Y. Li, Hybrid ground source heat pump system for overcoming soil thermal imbalance: a review, Sustain. Energy Technol. Assessments 44 (2021), 101098, https://doi.org/10.1016/j.seta.2021.101098.

[12] D.D. Cortes, A. Nasirian, S. Dai, Smart Ground-Source Borehole Heat Exchanger Backfills: A Numerical Study, International Symposium on Energy Geotechnics, Springer, 2018, pp. 27–34.

[13] D. Qi, L. Pu, F. Sun, Y. Li, Numerical investigation on thermal performance of ground heat exchangers using phase change materials as grout for ground source heat pump system, Appl. Therm. Eng. 106 (2016) 1023–1032, https://doi.org/10.1016/j.applthermaleng.2016.06.048.

[14] H. Qian, Y. Wang, Modeling the interactions between the performance of ground source heat pumps and soil temperature variations, Energy Sustain Dev 23 (2014) 115–121, https://doi.org/10.1016/j.esd.2014.08.004.

[15] H.-x. Liu, J. Yang, X. Zhang, X. Zhou, Analysis on optimal heating load ratio of hybrid ground source heat pump system in cold area, Chinese Journal of Refrigeration Technology (2012).

[16] L. Ni, W. Song, F. Zeng, Y. Yao, Energy Saving and Economic Analyses of Design Heating Load Ratio of Ground Source Heat Pump with Gas Boiler as Auxiliary Heat Source, 2011 International Conference on Electric Technology and Civil Engineering (ICETCE), IEEE, 2011, pp. 1197–1200.

[17] B. Zhang, Energy-efficiency evaluation of ground-source heat pump and ice thermal storage composite system for an office building, Building Energy Efficiency 1 (14–17) (2016) 25.

[18] M.-J. Hsiao, Y.-F. Kuo, C.-C. Shen, C.-H. Cheng, S.-L. Chen, Performance enhancement of a heat pump system with ice storage subcooler, Int. J. Refrig. 33 (2) (2010) 251–258, https://doi.org/10.1016/j.ijrefrig.2009.11.002.

[19] T. Başer, J.S. McCartney, Transient evaluation of a soil-borehole thermal energy storage system, Renew. Energy 147 (2020) 2582–2598, https://doi.org/10.1016/j.renene.2018.11.012.

[20] Y. Lin, Y. Jia, G. Alva, G. Fang, Review on thermal conductivity enhancement, thermal properties and applications of phase change materials in thermal energy storage, Renew. Sustain. Energy Rev. 82 (2018) 2730–2742.

[21] Y. Konuklu, M. Ostry, H.O. Paksoy, P. Charvat, Review on using microencapsulated phase change materials (PCM) in building applications, Energy Build. 106 (2015) 134–155, https://doi.org/10.1016/j.enbuild.2015.07.019.

[22] A. Datas, Silicon and ferrosilicon latent heat thermal batteries, Silicon for The Chemical Solar Industry XV (2020) 285.

[23] R. Sharma, E. Anil Kumar, P. Dutta, S. Srinivasa Murthy, Y.I. Aristov, M.M. Tokrev, T.X. Li, R.Z. Wang, Ammoniated salt based solid sorption thermal batteries: a comparative study, Appl. Therm. Eng. 191 (2021), 116875, https://doi.org/10.1016/j.applthermaleng.2021.116875.

[24] Z. Khan, Z. Khan, A. Ghafoor, A review of performance enhancement of PCM based latent heat storage system within the context of materials, thermal stability and compatibility, Energy Convers. Manag. 115 (2016) 132–158, https://doi.org/10.1016/j.enconman.2016.02.045.

[25] X. Huang, G. Alva, Y. Jia, G. Fang, Morphological characterization and applications of phase change materials in thermal energy storage: a review, Renew. Sustain. Energy Rev. 72 (2017) 128–145, https://doi.org/10.1016/j.rser.2017.01.048.

[26] M. Bottarelli, M. Bortoloni, Y. Su, C. Yousif, A.A. Aydın, A. Georgiev, Numerical analysis of a novel ground heat exchanger coupled with phase change materials, Appl. Therm. Eng. 88 (2015) 369–375, https://doi.org/10.1016/j.applthermaleng.2014.10.016.

[27] W.-l. Cheng, R.-m. Zhang, K. Xie, N. Liu, J. Wang, Heat conduction enhanced shape-stabilized paraffin/HDPE composite PCMs by graphite addition: preparation and thermal properties, Sol. Energy Mater. Sol. Cells 94 (10) (2010) 1636–1642, https://doi.org/10.1016/j.solmat.2010.05.020.

[28] J. Molefi, A. Luyt, I. Krupa, Comparison of LDPE, LLDPE and HDPE as matrices for phase change materials based on a soft Fischer–Tropsch paraffin wax, Thermochim. Acta 500 (1–2) (2010) 88–92, https://doi.org/10.1016/j.tca.2010.01.002.

[29] A. Yataganbaba, B. Ozkahraman, I. Kurtbas, Worldwide trends on encapsulation of phase change materials: a bibliometric analysis (1990–2015), Appl. Energy 185 (2017) 720–731, https://doi.org/10.1016/j.apenergy.2016.10.107.

[30] Y. Lin, Y. Jia, G. Alva, G. Fang, Review on thermal conductivity enhancement, thermal properties and applications of phase change materials in thermal energy storage, Renew. Sustain. Energy Rev. 82 (2018) 2730–2742, https://doi.org/10.1016/j.rser.2017.10.002.

[31] M. Aguayo, Phase Change Materials in Infrastructural Concrete and Buildings: Material Design and Performance, Arizona State University, 2018.

[32] J.L. Wang, J.D. Zhao, N. Liu, Numerical Simulation of Borehole Heat Transfer with Phase Change Material as Grout, Applied Mechanics and Materials, Trans Tech Publ, 2014, pp. 44–47.

[33] A.M. Abdulateef, M. Jaszczur, Q. Hassan, R. Anish, H. Niyas, K. Sopian, J. Abdulateef, Enhancing the melting of phase change material using a fins–nanoparticle combination in a triplex tube heat exchanger, J. Energy Storage 35 (2021), 102227, https://doi.org/10.1016/j.est.2020.102227.

[34] X. Li, C. Tong, L. Duanmu, L. Liu, Study of a U-tube heat exchanger using a shape-stabilized phase change backfill material, Science and Technology for the Built Environment 23 (3) (2017) 430–440, https://doi.org/10.1080/23744731.2016.1243409.

[35] P.K. Dehdezi, M.R. Hall, A.R. Dawson, Enhancement of Soil Thermo-Physical Properties Using Microencapsulated Phase Change Materials for Ground Source Heat Pump Applications, Applied Mechanics and Materials, Trans Tech Publ, 2012, pp. 1191–1198.

[36] S. Guichard, F. Miranville, D. Bigot, B. Malet-Damour, K. Beddiar, H. Boyer, A complex roof incorporating phase change material for improving thermal comfort in a dedicated test cell, Renew. Energy 101 (2017) 450–461, https://doi.org/10.1016/j.renene.2016.09.018.

[37] L. Navarro, A. De Gracia, D. Niall, A. Castell, M. Browne, S.J. McCormack, P. Griffiths, L.F. Cabeza, Thermal energy storage in building integrated thermal systems: a review. Part 2. Integration as passive system, Renew. Energy 85 (2016) 1334–1356, https://doi.org/10.1016/j.renene.2015.11.040.
[38] G. Panayiotou, S.A. Kalogirou, S.A. Tassou, Evaluation of the application of Phase Change Materials (PCM) on the envelope of a typical dwelling in the Mediterranean region, Renew. Energy 97 (2016) 24–32, https://doi.org/10.1016/j.renene.2016.05.043.
[39] C. Han, X.B. Yu, An innovative energy pile technology to expand the viability of geothermal bridge deck snow melting for different United States regions: computational assisted feasibility analyses, Renew. Energy 123 (2018) 417–427, https://doi.org/10.1016/j.renene.2018.02.044.
[40] M. Mousa, A. Bayomy, M. Saghir, Phase change materials effect on the thermal radius and energy storage capacity of energy piles: experimental and numerical study, Int. J. Thermofluids 10 (2021), 100094, https://doi.org/10.1016/j.ijft.2021.100094.
[41] S.R. Nicholson, L.R. Kober, P. Atefrad, A. Mwesigye, S.B. Dworkin, The influence of geometry on the performance of a helical steel pile as a geo-exchange system, Renew. Energy 172 (2021) 714–727, https://doi.org/10.1016/j.renene.2021.03.067.
[42] A.K. Sani, R.M. Singh, T. Amis, I. Cavarretta, A review on the performance of geothermal energy pile foundation, its design process and applications, Renew. Sustain. Energy Rev. 106 (2019) 54–78, https://doi.org/10.1016/j.rser.2019.02.008.
[43] J. Huang, J.S. McCartney, H. Perko, D. Johnson, C. Zheng, Q. Yang, A novel energy pile: the thermo-syphon helical pile, Appl. Therm. Eng. 159 (2019), 113882, https://doi.org/10.1016/j.applthermaleng.2019.113882.
[44] L. Bandeira-Neto, G. Narsilio, N. Makasis, R. Choudhary, Y. Carden, Thermal response of energy screw piles: a case study in Australia, J. Geotech. Geoenviron. Eng. (2022), https://doi.org/10.1061/jggefk/gteng-11082 [in press].
[45] A.B. Comsol, COMSOL Multiphysics v5.5, 2020. http://www.comsol.com.
[46] Y. Zhong, G.A. Narsilio, N. Makasis, C. Scott, Experimental and numerical studies on an energy piled wall: the effect of thermally activated pile spacing, Geomech, Energy Environ. 29 (2022), 100276, https://doi.org/10.1016/j.gete.2021.100276.
[47] A. Bidarmaghz, 3D Numerical Modelling of Vertical Ground Heat Exchangers, The Department of Infrastructure Engineering, The University of Melbourne, Melbourne, Australia, 2014.
[48] N. Makasis, Further Understanding Ground Source Heat Pump System Design Using Finite Element Methods and Machine Learning Techniques, The Department of Infrastructure Engineering, The University of Melbourne, Melbourne, Australia, 2018.
[49] Y. Liu, D.D. Cortes, X.B. Yu, G. Narisio, S. Dai, Numerical investigations of enhanced shallow geothermal energy recovery using microencapsulated phase change materials and metal fins, Acta Geotech (2022) [under review].
[50] H.A. Adine, H. El Qarnia, Numerical analysis of the thermal behaviour of a shell-and-tube heat storage unit using phase change materials, Appl. Math. Model. 33 (4) (2009) 2132–2144, https://doi.org/10.1016/j.apm.2008.05.016.
[51] A. Karaipekli, A. Biçer, A. Sarı, V.V. Tyagi, Thermal characteristics of expanded perlite/paraffin composite phase change material with enhanced thermal conductivity using carbon nanotubes, Energy Convers. Manag. 134 (2017) 373–381, https://doi.org/10.1016/j.enconman.2016.12.053.
[52] T. Armour, P. Groneck, J. Keeley, S. Sharma, Micropile Design and Construction Guidelines: Implementation Manual, United States, Federal Highway Administration, 2000.